Biosensors and Bioelectronics 267 (2025) 116839

Contents lists available at ScienceDirect

Biosensors and Bioelectronics

journal homepage: www.elsevier.com/locate/bios

Ultrasensitive detection of cancer-associated nucleic acids and mutations by primer exchange reaction-based signal amplification and flow cytometry

Samet Kocabey [a,b,*], Sarah Cattin [a,b,c], Isabelle Gray [a,b], Curzio Rüegg [a,b,**]

[a] Laboratory of Experimental and Translational Oncology, Department of Oncology, Microbiology and Immunology, Faculty of Science and Medicine, University of Fribourg, Chemin Du Musée 18, PER17, 1700, Fribourg, Switzerland
[b] NCCR Bio-inspired Materials, University of Fribourg, 1700, Fribourg, Switzerland
[c] Cell Analytics Facility, Faculty of Science and Medicine, University of Fribourg, Chemin Du Musée 18, PER17, 1700, Fribourg, Switzerland

ARTICLE INFO

Keywords:
DNA biosensor
Primer exchange reaction
Signal amplification
Flow cytometry
Cancer detection
Single-nucleotide mutation
ctDNA
RNA

ABSTRACT

The detection of cancer-associated nucleic acids and mutations through liquid biopsy has emerged as a highly promising non-invasive approach for early cancer detection and monitoring. In this study, we report the development of primer exchange reaction (PER) based signal amplification strategy that enables the rapid, sensitive and specific detection of nucleic acids bearing cancer specific single nucleotide mutations using flow cytometry. Using micrometer size beads as support for immobilizing oligonucleotides and programmable PER assembly for target oligonucleotide recognition and fluorescence signal amplification, we demonstrated the versatile detection of target nucleic acids including *KRAS* oligonucleotide, fragmented mRNAs, and miR-21. Moreover, our detection system can discriminate single base mutations frequently occurred in cancer-associated genes including *KRAS*, *PIK3CA* and *P53* from cell extracts and circulating tumor DNAs (ctDNAs). The detection is highly sensitive, with a limit of detection down to 27 fM without pre-amplification. In view of a clinical application, we demonstrate the detection of single mutations after extraction and pre-amplification of ctDNAs from the plasma of breast cancer patients. Importantly, our detection strategy enabled the detection of single *KRAS* mutation even in the presence of 1000-fold excess of wild type (WT) DNA using multi-color flow cytometry detection approach. Overall, our strategy holds immense potential for clinical applications, offering significant improvements for early cancer detection and monitoring.

1. Introduction

Cancer is one of the main leading causes of mortality worldwide and remains a major public health challenge (Mehlen and Puisieux, 2006). Many of the screening methods applied for the early detection of cancer are either ineffective, expensive, or highly invasive, and thus only performed on a minority of people, or only after the appearance of symptoms. Tissue biopsy remains an essential technique that is invaluable to confirm diagnosis and determine the nature of the cancer, however it has intrinsic limitations: it is an invasive procedure that is applicable only when the lesion is visible (clinically through imaging methods), is challenging to repeat, it provides only a limited number of specimens for further genetic testing, and it may pose a risk for the patient as some tumors are difficult to access due to their anatomical location (Perakis and Speicher, 2017; Tanaka et al., 2017). The discovery of tumor-derived biomarkers in plasma and other body fluids of cancer patients has emerged as a new approach known as liquid biopsy (Lone et al., 2022). Liquid biopsy is being considered as a minimally invasive tool that may be rapidly used for cancer detection at an early stage (Wan et al., 2017). It may also be used to validate the efficiency of a cancer treatment by taking multiple samples in the following weeks and months for the monitoring of cancer patients for relapse.

Liquid biopsy obtained from peripheral blood encompasses different tumoral components including circulating tumor cells (CTCs), circulating tumor DNA (ctDNA), extracellular vesicles (EVs), mRNAs and micro-RNA (miRNA) (Siravegna et al., 2017). These elements can be

* Corresponding author. Laboratory of Experimental and Translational Oncology, Department of Oncology, Microbiology and Immunology, Faculty of Science and Medicine, University of Fribourg, Chemin du Musée 18, PER17, 1700, Fribourg, Switzerland.
** Corresponding author. Laboratory of Experimental and Translational Oncology, Department of Oncology, Microbiology and Immunology, Faculty of Science and Medicine, University of Fribourg, Chemin du Musée 18, PER17, 1700 Fribourg, Switzerland.
E-mail addresses: samet.kocabey@unifr.ch (S. Kocabey), curzio.ruegg@unifr.ch (C. Rüegg).

https://doi.org/10.1016/j.bios.2024.116839
Received 23 April 2024; Received in revised form 27 September 2024; Accepted 4 October 2024
Available online 5 October 2024

isolated for the identification of various tumor-specific genomic aberrations including point mutations, copy number variations, structural rearrangements, or epigenetic patterns (Palacin-Aliana et al., 2021). The level of circulating nucleic acids (ctDNAs, mRNAs and miRNAs) were found to be elevated in a broad spectrum of cancer types relative to healthy individuals and the expression can be further altered during the progression of the particular cancer type (Kosaka et al., 2010). Moreover, the cancer specific mutations (e.g. *KRAS* mutation) that were detected in the patient's blood were found to be identical in the patient's tumor, thereby confirming that the mutant DNA fragments in the plasma were of tumor origin and reflects therefore tumor genetics (Sorenson et al., 1994). After the approval of the first liquid biopsy test developed by Roche (EGFR mutation test) in 2016 (Kwapisz, 2017), the United States Food and Drug Administration (FDA) has granted approval for diagnostic tests and many companies started the development of liquid biopsy tests for the early detection, prognosis, and post-treatment monitoring of cancer (e.g. Qiagen therascreen kits, Galleri MCED test) (Duffy and Crown, 2023; Vallee et al., 2014).

Considering the fact that the concentration of circulating nucleic acids in the bloodstream could be in the range of low femtomolar (fM) concentrations, sensitive and specific detection methods are urgently needed for precise cancer diagnostics (Elazezy and Joosse, 2018; Shin et al., 2023; Williams et al., 2013). Common detection techniques involve complex, expensive and time-consuming approaches such as next-generation sequencing (NGS), digital PCR (dPCR) or microarray hybridization (Song et al., 2022). Although these sensing techniques enable high-throughput detection of multiple nucleic acids, they can suffer from low sensitivity and low specificity, especially when detecting highly homologous sequences that can differ by a single nucleotide due to cross-hybridization, and reliable detection of mutations below 1% could be challenging due to amplification and sequencing errors (Song et al., 2022).

In this regard, DNA nanotechnology approaches offer promising tools for the detection of cancer biomarkers, including CTCs (Rafiee et al., 2020), cell free RNA and DNA (Domljanovic et al., 2022; Kocabey et al., 2023), or cellular membrane proteins (Sun et al., 2022). Very recently, a variety of signal amplification strategies have been developed to enhance the sensitivity of cancer biomarker detection including deoxyribozymes (DNAzyme) (McConnell et al., 2021), catalyzed hairpin assembly (CHA) (He et al., 2024), rolling circle amplification (RCA) (Li et al., 2023) and hybridization chain reaction (HCR) (Lazaro et al., 2022). However, many of these strategies mainly rely on an on-going reaction and they are incompatible with a ready-to-use design with higher controllability (Huang et al., 2023). Moreover, the *in situ* enzymatic reaction could be hard to control or tune for individual targets. By contrast, primer exchange reaction (PER) allows automated and programmable one-step synthesis of the long single-stranded DNA (ssDNA) concatemer for sensitive, *in situ* enzymatic reaction-free and highly multiplexed biosensing and bioimaging in a prescribed fashion (Kishi et al. 2018, 2019). It is based on a catalytic hairpin reaction in the presence of polymerase with exonuclease activity and branch migration, which allows controlled extension of a short primer sequence in an iterative manner through binding to the complementary hairpin strand (Saka et al., 2019). The simple step-by-step synthesis offers high programmability, tight control of the reaction by external parameters including hairpin or dNTP concentration, reaction time and temperature, and allows producing long DNA concatemers of desired lengths.

In this study, we demonstrate a facile and rapid PER-based signal amplification technique for the sensitive and specific detection of cancer-associated nucleic acids and mutations using flow cytometry. The detection is based upon the direct one-step binding of target RNA/DNA strand to the bead-immobilized counterpart and PER elongated concatemer, which enabled very sensitive detection at low femtomolar concentrations without amplification. We point out that the sensor can detect fragmented mRNAs and miRNAs from cancer cell extracts and more importantly, the detection of ctDNAs isolated from the blood (plasma) of breast cancer patients. Importantly, the sensor can effectively discriminate single-base mutations frequently present in ctDNAs after pre-amplification indicating the great prospect in precision required for the development of a liquid biopsy tool for early detection and monitoring of cancers.

2. Materials & methods

2.1. Materials

All unmodified and biotin modified DNA oligonucleotides were ordered from LubioScience-Switzerland IDT (Zurich, Switzerland). Alexa-488 and Alexa-647 modified imager DNA strands (HPLC purified) were purchased from Eurofins MWG Operon (Ebersberg, Germany). Synthetic miRNAs and RNA oligonucleotides were purchased from Microsynth AG (Balgach, Switzerland). The detailed sequences of the oligonucleotides are given in Table S1. Streptavidin coated polystyrene beads (6–6.9 μm diameter) were obtained from Spherotech, Illinois, USA. Bst DNA polymerase (M0275L, 8000 U/mL), $MgSO_4$ (100 mM), ThermoPol® reaction buffer, deoxynucleotide (dNTP) solution mix (N0447S), RNase H (M0297S), HiScribe T7 High Yield RNA Synthesis Kit (E2040S) and Monarch® RNA Cleanup Kit (T2050L, 500 μg) were purchased from New England Biolabs (NEB) (Ipswich, MA, USA). NucleoSpin® Gel and PCR Clean-up kit (740609.50), cfDNA isolation kit (cfDNA XS, 740900.50) and RNA isolation kit (NucleoSpin® RNA plus) were purchased from Macherey-Nagel. High Pure miRNA isolation kit was purchased from Roche. Taq DNA polymerase (cat: 10342053), SYBR safe DNA gel stain (10x, cat: S33102), GeneRuler DNA ladder mix (cat: SM0331), RiboRuler RNA ladders (cat: SM1821 and SM1831) and all cell culture reagents were ordered from Thermo Fisher Scientific (Basel, Switzerland).

2.2. Preparation of PER concatamers

PER concatemers were prepared based on a previous method with slight modification (Saka et al., 2019). Typically, 100 μL reactions were prepared in 1x ThermoPol reaction buffer (diluted from 10x stock) with final concentrations of 10 mM MgSO4, 400 U/mL of Bst LF polymerase, 600 μM each of dATP, dCTP, and dTTP, 100 nM of Clean G hairpin and 0.15 μM of hairpin for target oligonucleotide. After addition of water to 99 μL and the reaction mixture was incubated for 15 min at 37 °C, followed by the addition of 1 μL of 100 μM primer (Xp) to obtain 1 μM final concentration, and the reaction was incubated for another 1–3 h at 37 °C. The reaction was terminated by heating to 80 °C for 20 min to deactivate the polymerase.

2.3. Isolation of RNAs from human cells and cfDNAs from human plasma

Human cancer cell lines (MCF-7, MDA-MB-231 and A549) were cultured at 37 °C, 5% CO_2 and 95% humidity in Dulbecco's modified Eagle's medium (DMEM) supplemented with Glutamax, 10% fetal bovine serum (FBS), and 1% Penicillin and Streptomycin. mRNA isolation from these cell lines was performed using the NucleoSpin® RNA plus RNA isolation kit (10^6 cells). Extraction was done as described in the kit protocol. To isolate miRNAs from cells, the column protocol for the isolation of the small RNA was applied as described in the High Pure miRNA isolation kit. To detect circulating DNAs from human blood samples, 240 μL of plasma was used for each sample (8 samples from breast cancer patients and 3 samples from healthy donors). CtDNAs were extracted using NucleoSpin cfDNA isolation kit. Previously collected plasma samples were used in this study (Cattin et al., 2021). Ethical approval was obtained from the Cantonal ethic commission for human research on Humans of the Canton Ticino (CE 2967) and extended to Vaud-Fribourg-Neuchatel (Switzerland).

2.4. CDNA synthesis, PCR, in vitro transcription (IVT) and RNase H cleavage

Isolated RNA samples were reversely transcribed into cDNAs using the High-Capacity cDNA Reverse Transcription kit. First, 10 μL of 2x RT master mix was prepared according to the kit protocol and mixed with 10 μL (1 μg) of RNA isolate from cells for each sample. Samples were then incubated in a thermal cycler (Biometra TAdvanced, Analytik Jena) at 37 °C for 2 h followed by 85 °C for 5 min to inactivate the enzymes and immediately cooled down to 4 °C. Once the cDNA synthesis was completed, 2 μL of cDNA template was mixed with 2 μL of 10x Taq polymerase reaction buffer, 0.8 μL of $MgCl_2$ (2 mM), 0.4 μL of dNTP mix (200 μM), 0.4 μL of forward primer with T7 RNA polymerase binding site (10 μM), 0.4 μL of reverse primer (10 μM), 0.2 μL of Taq DNA polymerase and 13.8 μL of RNase-free water for PCR reaction. Samples were incubated in the thermal cycler with a temperature profile of 95 °C for 3 min, followed by 35 amplification cycles (95 °C for 20 s, 58 °C for 40 s, and 72 °C for 40 s), and a final extension at 72 °C for 10 min. The primer sequence is provided in Table S1.

For the amplification of target mRNAs (actin, vimentin, *KRAS*, *PIK3CA* and *P53*), 2 μL of PCR product was mixed with 2 μL of 10x reaction buffer, 8 μL of NTP mix (ATP, GTP, CTP, UTP, 10 mM each), 1 μL of DTT (5 mM) and 2 μL of T7 RNA polymerase mix and completed up to 20 μL with RNase free water as described in the protocol of HiScribe T7 High Yield RNA Synthesis Kit. The solution was incubated in the thermal cycler at 37 °C for 2 h. After incubation, synthesized RNA was purified using Monarch® RNA Cleanup Kit.

Fragmentation of mRNAs and transcribed RNAs were done using RNase H enzyme. For this, guide oligonucleotides (20 nt single-stranded DNA) were first designed to bind upstream and downstream on the specific regions in the target RNA sequence (see Fig. S2). Then, transcribed RNA sample (5 μg) or cell isolated total RNA (20 μg) was mixed with 2 μL of guide oligonucleotides (1 μM each), completed up to 19,5 μL with RNase free water and heated it to 70 °C for 5 min for DNA:RNA hybridization. Then, 0,5 μL of RNase H was added, mixed and heated for 2 h at 37 °C to allow the enzyme to cut RNA in the DNA:RNA hybrid for the release of the target RNA for detection. Finally, RNase H was inactivated by incubation at 65 °C for 10 min. For the detection of miR-21, 600 ng of cell-extracted small RNA solution was used.

2.5. Detection of target RNAs by flow cytometry

20 μL of streptavidin coated polystyrene beads (6–6.9 μm diameter, 0.5% w/v) were transferred to V-bottom 96-well microplate (Thermo Fisher Scientific (Basel, Switzerland)) and completed up to 100 μL with 1x PBS. The solution was centrifuged at 2000 rpm (Awel MF48-R) for 5 min and the supernatant removed completely. Then, the plate was placed on ice and the beads were incubated sequentially with biotinylated oligonucleotide (100 nM) for 30 min, target RNA containing solution for 30 min, 20 μL of primary PER solution for 30 min, 20 μL of secondary PER solution for 30 min (for branched amplification) and imager strand (1 μM) for 30 min in 100 μL of 1x PBS. Between each step, the beads were rinsed with 100 μL of 1x PBS and centrifuged at 2000 rpm for 5 min to wash unbound molecules away. After incubation for the respective times, the beads were analyzed using Cytek Aurora flow cytometer (Figs. 2 and 3) or MACSQuant Analyzer 10 flow cytometer (Miltenyi Biotec) (Figs. 4 and 5). All flow cytometers were calibrated using specific QC beads and protocol, and instrument setting were standardized using the obtained gain and minimal aspiration speed. For Cytek Aurora, unmixing was done using proper reference and unstained controls with autofluorescence extraction. Data was analyzed with FlowJo Software (v10, FlowJo LLC). Mean fluorescence intensity (MFI) for all samples were background corrected by subtracting the MFI values from the appropriate controls.

3. Results and discussion

3.1. PER-based detection principle

To achieve the fast and ultrasensitive detection of cancer-associated nucleic acids including mRNAs, miRNAs and ctDNAs that carry cancer driver mutations, we developed a DNA-based sensor consisting of a programmable PER assembly mediating fluorescence signal amplification detectable by flow cytometry. For this, we used streptavidin-coated

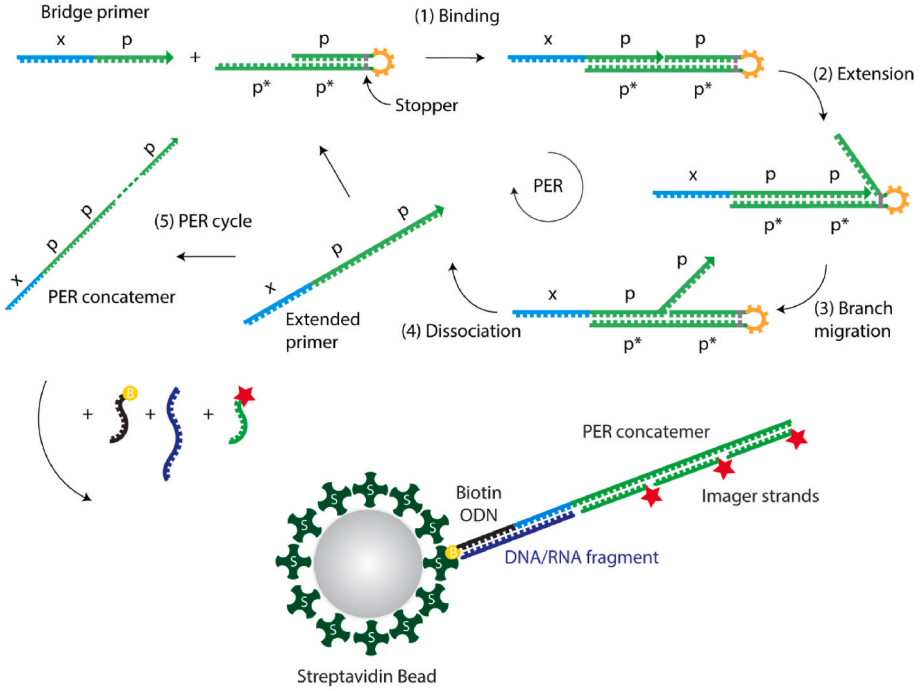

Fig. 1. Schematic illustration of the programmable PER assembly and the detection of cancer-associated DNAs or RNAs using PER-based signal amplification technique.

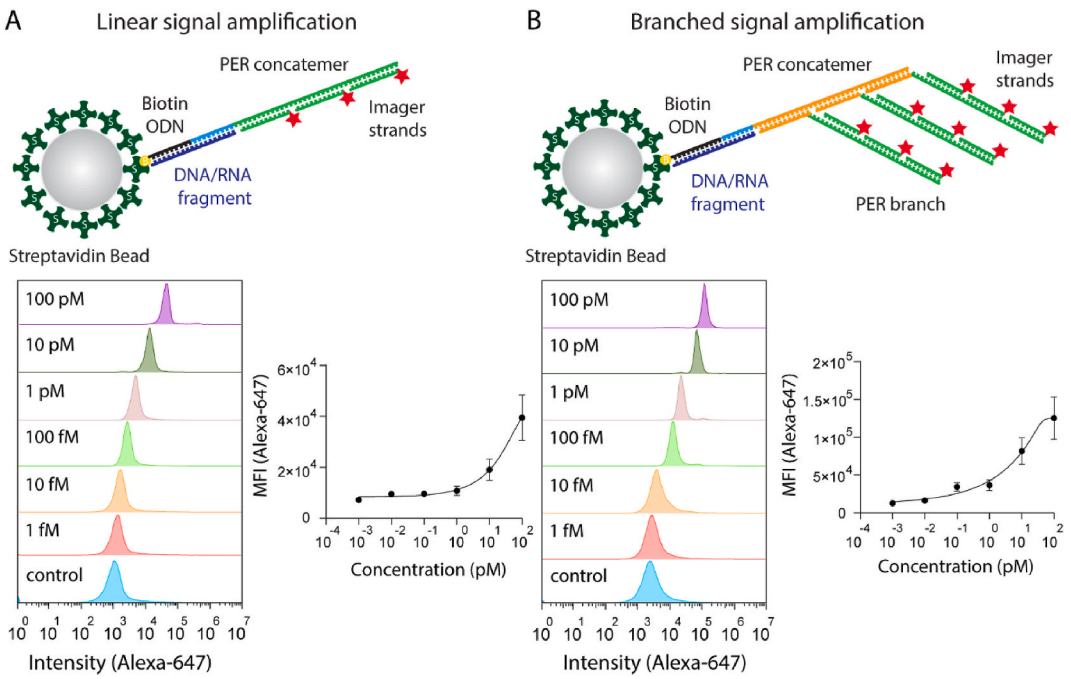

Fig. 2. Detection of *KRAS* DNA oligonucleotide at the concentrations of 1 fM to 100 pM using A) linear signal amplification and B) branched signal amplification approaches. At least 20,000 events were recorded to calculate MFIs using Cytek Aurora flow cytometer.

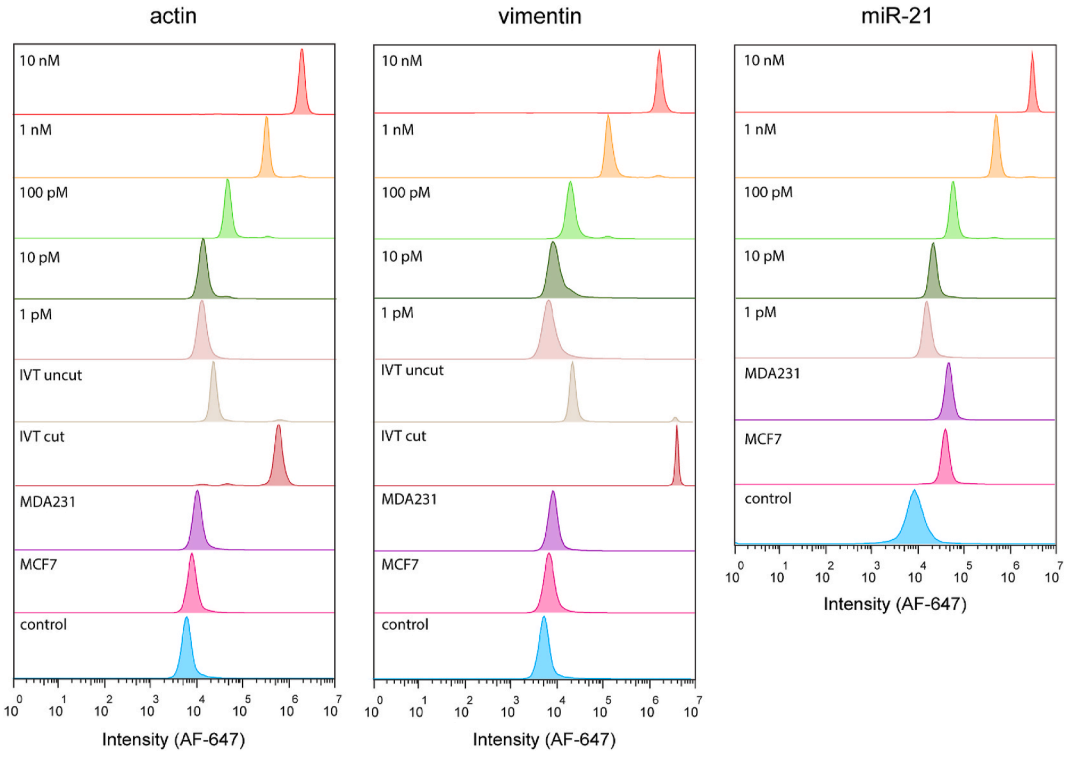

Fig. 3. Detection of actin and vimentin mRNAs and miR-21 from cancer cell extracts using PER-based branched signal amplification. Synthetic single strand RNA oligonucleotides were used at the concentrations of 1 pM–10 nM to calculate the detection sensitivity. At least 30,000 events were recorded to calculate MFIs using Cytek Aurora flow cytometer. IVT cut: *in vitro* transcribed and cleaved by RNase H, IVT uncut: *in vitro* transcribed but not cleaved by RNase H.

beads with a diameter of 6 μm to provide a defined and stable support for immobilizing biotinylated oligonucleotide to start the hybridization cascade. The biotinylated oligonucleotide is designed in a way that the target oligonucleotide can bind partially to the immobilized biotinylated oligonucleotide. The remaining single-stranded unhybridized part of the target oligonucleotide is designed to form a duplex with the x domain of the bridge primer (xp) (Fig. 1). To assemble the PER concatemer which recognizes the target oligonucleotide, the bridge primer first binds (1) to the p* domain of the respective hairpin oligonucleotide and extended (2) isothermally in the presence of strand-displacing DNA polymerase

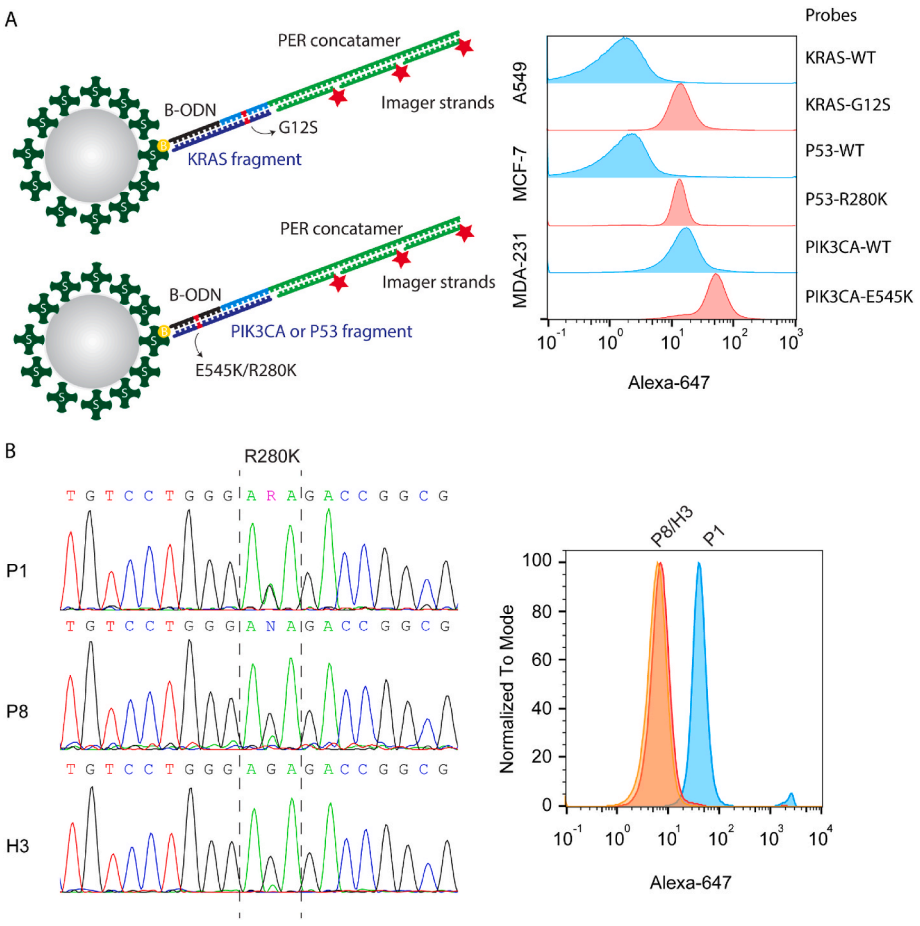

Fig. 4. A) Detection of single mutations (KRAS-G12S, P53-R280K and PIK3CA-E545K) from cancer cell extracts using PER-based linear signal amplification. B) Detection of P53-R280K mutation after extraction of ctDNAs from the plasma of breast cancer patients and healthy donors. At least 27 × 10^4 events were recorded to calculate MFIs using MACSQuant flow cytometer.

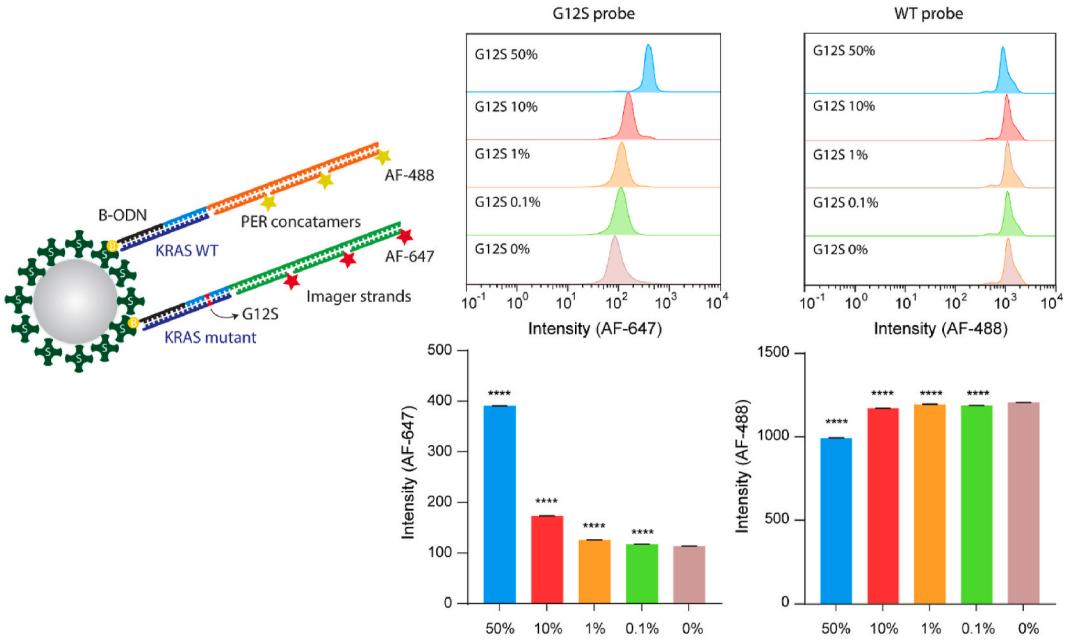

Fig. 5. Multicolor detection of *KRAS* G12S mutation in the background of *KRAS* wild-type DNA fragment. AF-647 labelled imager strands were used for G12S probe and AF-488 labelled imager strands were used for WT probe. At least 29 × 10^4 events were recorded to calculate MFIs using MACSQuant flow cytometer. Statistical analysis was performed by an unpaired *t*-test (****$p < 0.0001$).

until encountering with the stopper base-pair. The stopper is made of a G-C pair and the on-going polymerization halts at this point due to lack of dGTP in the solution, which induces the dissociation of the newly synthesized sequence (xpp) from the hairpin through the branch migration (3). This leads to spontaneous separation between the extended primer and hairpin (4). After this separation, the extended primer (xpp) re-joins a next cycle for further elongation (5). Finally, a long ssDNA concatemer with repeated p domains formed after many PER cycle. To achieve fluorescence signal amplification, the PER-derived DNA concatemer is further hybridized to fluorophore labelled imager strands directly for linear amplification or through to secondary concatemers and then to fluorescent imager strands for branched signal amplification. The generation of PER concatemers and hybridization of imager strands were verified by gel analysis (Fig. S1).

3.2. Determining the detection sensitivity

Next, we performed flow cytometry for the detection of target DNA oligonucleotide using PER assembly strategy. As a proof-of-concept experiment, we used a synthetic single stranded DNA fragment of human *KRAS* proto-oncogene for the detection with a linear and branched fluorescence signal amplification approaches. Initially, we tested different flow cytometers that are both conventional and full spectrum technology (some of them are commonly used in the clinics, e.g. BD FACS Canto II) and available at our facility (Cytek Aurora, BD FACS Canto II, BD LSR Fortessa and MACSQuant Analyzer) to compare the detection sensitivities based on their internal parameters (e.g. laser power) (Fig. S2). For this, we applied target oligonucleotide concentrations in the range from 100 nM to 100 fM. Among these systems, we achieved the highest sensitivity using the full spectrum flow cytometer Cytek Aurora in which we could detect 100 fM of oligonucleotide with linear fluorescence amplification, whereas the detection limit using MACSQuant flow cytometer was reached at 10 pM. The detection sensitivities obtained by using both BD instruments (Canto II and LSR Fortessa) were similar with a detection limit of 1 pM and less sensitive compared to Cytek Aurora. Therefore, we utilised Cytek Aurora flow cytometer for the sensitivity experiments. To calculate the detection sensitivity using linear signal amplification method, we incubated the beads in the buffer solutions containing different concentrations of target oligonucleotides ranging from 100 pM to 1 fM as shown in Fig. 2A. Flow cytometry analysis with a linear signal amplification demonstrated that the binding of *KRAS* oligonucleotide is maximal, with a mean fluorescence intensity (MFI) of 3.95 x 10^4 when 100 pM of oligonucleotide was added to the beads and the binding of *KRAS* oligonucleotide was gradually decreased down to the concentration of 1 fM, with an MFI of 7.24 x 10^4. The MFI without target oligonucleotide was measured as 7.45 x 10^4. The theoretical limit of detection (LoD) of target oligonucleotides was defined as the mean fluorescence intensity plus three standard deviations (3 σ) of the blank sample. By fitting all the measured data points (100 pM–1 fM) to an asymmetric five-parameter curve, the LoD of *KRAS* oligonucleotide was determined as 94 fM.

In order to provide further signal enhancement, we used a sequential amplification strategy where independently assembled secondary concatemers can be hybridized and branched off the primary concatemers so that more binding sites for fluorescent imager strands are generated (Fig. 2B). Compared to linear signal amplification, the fluorescence intensity generated by branched signal amplification (Fig. 2B) was increased up to 3.17-fold at the concentration of 100 pM target oligonucleotide (MFI: 1.25 x 10^5) and 3.57-fold at the concentration of 100 fM of target oligonucleotide (MFI: 3.43 x 10^4). Using the same formula generated from the asymmetric curve, the LoD of *KRAS* oligonucleotide using branched signal amplification was determined as 27 fM. With respect to unamplified signal, the linear PER assembly method yielded 75-fold signal amplification and branched PER assembly method yielded 284-folds signal amplification (Fig. S3). The amplification levels were comparable with previous studies where PER-based signal amplification was applied for *in situ* hybridization on fixed samples (Saka et al., 2019). We also tried to further amplify the signal by adding tertiary concatemers, but the fluorescence signal only enhanced 11-fold compared to the unamplified signal. This could be attributed to the lack of incorporation efficiency of the tertiary concatemers due to the steric hindrance and the repulsion generated by high amount of negatively charged DNA backbones in the solution (Soleymani et al., 2011).

3.3. Detection of target RNAs from cell extracts

We next aimed to investigate the detection of target RNAs using our PER-based branched signal amplification approach. To this end, we chose three different target RNAs for a proof-of-concept experiment: 1) actin mRNA, the housekeeping gene encoding actin cytoskeleton protein, 2) vimentin mRNA, a marker of epithelial to mesenchymal transition (EMT), and 3) miR-21, an oncogenic miRNA highly expressed in several cancer types. Initially, to estimate the detection sensitivity of our approach for RNA targets, we incubated the beads separately with the synthetic RNA fragments of the corresponding target RNAs (actin-RF: 30 nt, vimentin-RF: 32 nt and miR-21: 22 nt, the sequences are given in Table S1) using different concentrations of target RNAs ranging from 10 nM to 1 pM (Fig. 3A). All of target RNAs were detectable at the concentration of 1 pM ($MFI_{actin:}$ 19.9 × 10^3, $MFI_{vimentin:}$ 23 × 10^3, $MFI_{miR21:}$ 29.3 × 10^3). Then, to expand the detection capability of our sensing approach, we extracted cell-derived mRNAs and miRNAs from the human breast cancer cell lines MCF-7 and MDA-MB-231. First, for the detection of target mRNAs, we conducted RT-PCR and T7 transcription to amplify and generate large quantities of the actin and vimentin mRNAs. Agarose gel analysis revealed the successful production of transcripts *in vitro* with desired lengths (actin mRNA: 633 nt and vimentin mRNA: 718 nt) (Figs. S4A and B). We observed that when long target mRNA strands were directly incubated on our beads (depicted in Fig. 3 as IVT uncut), the obtained signal was lower than expected even though the initial mRNA amount is high (MFI_{actin}: 59 × 10^3 and $MFI_{vimentin}$: 23.4 × 10^4). This is most likely due to the secondary structure formation of transcribed mRNAs masking the target sequence thereby interfering with the efficient capture of the target RNA (Boskovic et al., 2023). To avoid this problem, we developed a targeted cutting of target mRNA using ribonuclease (RNase) H. The guide oligonucleotides (ssDNA, 20 nt) were designed to bind upstream and downstream on the specific (capture) regions of the target mRNAs (Fig. S4A). Then, RNase H was used to digest the RNA sequence in DNA:RNA hybrids thereby inducing the release of the target RNA fragment in the middle. The bands visualized in the agarose gel confirmed the production of the respective RNA fragments of actin and vimentin (Fig. S4C). After cutting with RNase H, the signal obtained from the beads incubated with fragmented target RNAs increased by an order of magnitude. The mean fluorescence intensity of actin fragment was 9.62-fold higher than fluorescence intensity of the uncut actin mRNA ($MFI_{actin\text{-}cut}$: 5.72 × 10^5) and the mean fluorescence intensity of vimentin fragment was 17.4-fold higher than the signal obtained from the uncut mRNA ($MFI_{vimentin\text{-}cut}$: 4.07 × 10^6). With these experiments, we demonstrated that targeted cutting of long mRNA strands into shorter fragments further increased the detection capacity of the PER-based signal amplification approach (Fig. 3).

After the successful detection of *in vitro* transcribed and fragmented target RNAs, we performed the direct detection of selected target RNAs from the cell extracts without any pre-amplification steps. For this purpose, extracted RNAs were mixed with respective guide oligonucleotides for actin and vimentin. After cutting with RNase H and incubating the solution containing fragmented RNAs with beads, branched signal amplification was applied. The results demonstrated the detection of actin and vimentin RNA fragments in the range of 0.3 pM–0.45 pM. The concentration of actin was higher in both cell lines compared to vimentin (MDA-MB-231: 0.45 pM, MCF-7: 0.37 pM). The concentration of vimentin is slightly higher in MDA-MB-231 cells (0.32 pM) compared

to the MCF-7 cells (0.3 pM) (Fig. 3). Then, for the detection of miR-21, we incubated the beads with a solution containing cell-extracted small RNA. The results demonstrated that the concentration of miR-21 was high in both cancer cell lines (MDA-MB-231: 48.2 pM and MCF-7: 40.3 pM). It is important to note that, similar expression patterns of actin and vimentin mRNA were also observed by qRT-PCR (Fig. S5). The small discrepancy for the expression of miR-21 between the two methods could be due to the amplification of homologous miRNAs by mismatch-tolerant qRT-PCR. Overall, these experiments demonstrated the feasibility of amplification-free detection of highly expressed RNAs using PER-based branched signal amplification. We can foresee that through the further optimization of the entire detection system, for example, by specifically adjusting the *in vitro* transcription time (Yu et al., 2023), even lower concentrations of RNA targets (1 zM to 1 fM) could be detected with pre-amplification.

3.4. Detection of single-nucleotide mutations from cell extracts and human plasma

To assess the specificity of our PER-based detection approach, we next investigated the ability to discriminate wild type sequences from single nucleotide mutations that occur frequently in cancer. Plasma ctDNAs carrying these mutations originated from the cancer cells serve as significant and reliable cancer biomarkers in liquid biopsy but their concentrations in the bloodstream of cancer patients is extremely low and are mixed with ctDNA fragments of wild-type sequences derived from normal cells (Elazezy and Joosse, 2018). To determine the ctDNA detection capability of our sensing approach, we first screen the genetic lesions for the common mutations that are found in several cancer types by PCR and Sanger sequencing. Among these mutations, the Gly-12 codon (G12) in *KRAS* (GGT) is a site of multiple base changes observed in cancer (Zhang et al., 2022). The *KRAS* G12S is a prominent cancer driver mutation, accounting for 4.4 % of all *KRAS* mutations that has been observed, including in 2.5% of non-small-cell lung cancer (NSCLC) and 2.8% of colorectal adenocarcinoma (Consortium, 2017; O'Bryan, 2019). Moreover, *PIK3CA* mutations (e.g. E542K, E545K) are common activating mutations in breast cancer (occurring in 20–30% of all cases) and are potent predictive markers for responses to PI3K inhibitors in Estrogen Receptor-Positive, HER2-Negative (ER^+/$HER2^-$) breast cancers (Shimoi et al., 2018). In addition to this, *P53* mutants (e.g., R248Q, R273H, and R280K) can be classified as contact mutants associated with breast cancer, particularly ER^-, that are involved in DNA binding without causing protein unfolding but inhibit its transcriptional activity (Gomes et al., 2018). To screen for these genetic alterations, we isolated the RNAs from lung (A549) and breast cancer cell lines (BT-474, MDA-MB-231 and MCF-7) and the transcripts including target mutations were amplified by RT-PCR. After sequencing of these regions (the sequences are given in Table S2), we observed that the *KRAS* G12S mutation is present only in A549 cells, whereas *PIK3CA* E545K and *P53* R280K mutations are present in ER^+/$HER2^-$ and ER^-/$HER2^-$ breast cancer cells, MCF-7 and MDA-MB-231 respectively. Then, to detect these mutations using the PER-based approach, we first *in vitro* transcribed the amplified regions and incubated the purified RNA strands with respective guide oligonucleotides for RNase H cleavage. After cleavage, the fragmented RNA strands carrying mutations (18–23 nt, the sequences are given in Table S1) were separately incubated on the beads covered with respective biotinylated oligonucleotides (WT or mutant probes). The *KRAS* mutation was located in the region (10 nt) that hybridizes to the PER concatemer, whereas *P53* and *PIK3CA* mutations were located in the regions (9 nt and 11 nt respectively) that hybridize to the biotinylated oligonucleotides. The beads were further incubated with PER concatemers complementary to the target fragments and the fluorescence intensities were recorded using MACSQuant flow cytometer. For the wild-type and mutant probes, two different biotinylated oligonucleotides were used for *P53* and *PIK3CA* RNAs and two different PER concatemers were used for *KRAS* RNA. The results showed that the fluorescence intensities were significantly higher in all conditions when the fragmented RNAs of target regions incubated with mutant probes ($MFI_{KRAS\text{-}WT}$: 2.16, $MFI_{KRAS\text{-}G12S}$: 18.7, $MFI_{P53\text{-}WT}$: 3.84, $MFI_{P53\text{-}R280K}$: 16.2, $MFI_{PIK3CA\text{-}WT}$: 31.9, $MFI_{PIK3CA\text{-}E545K}$: 65.5) (Fig. 4A). The signal obtained from *PIK3CA*-WT is higher compared to the other wild-type signals, which is probably due to the presence of two different alleles (heterozygosity) for *PIK3CA* gene in MCF-7 cells (Table S2). Overall, we demonstrated that we could efficiently distinguish the abovementioned cancer-specific mutations using PER-based signal amplification approach. By redesigning the probes and biotinylated oligonucleotides, other cancer driver mutations can be efficiently detected using our approach.

As we have characterized the detection specificity of our system on cellular extracts, we then employed this technique to identify ctDNAs with target mutations from the plasma of breast cancer patients. For this, we extracted ctDNAs from the plasma of the 8 patients with early, non-metastatic, breast cancer and 3 age-matched healthy donors for a proof-of-concept experiment. First, we amplified the *P53* gene for all samples and sequenced the amplicons using Sanger sequencing. After screening of all samples, we observed a heterozygous R280K mutation in the ctDNA extracted from one of the patient plasma samples (P1), whereas none of the ctDNAs extracted from the healthy individuals carry the respective mutation. The sequencing results were given in Table S3. Then, to distinguish these mutations using PER-based approach, we produced the respective RNA strands from three ctDNA samples (P1, P8 and H3) by *in vitro* transcription from the amplified regions and mixed the purified RNA strands with guide oligonucleotides for RNase H cleavage. After cleavage, PER-based linear signal amplification was applied by incubating fragmented RNAs on the beads and the fluorescence signal was recorded with MACSQuant flow cytometer. The results showed that we can specifically detect the heterozygous mutation located in the R280K codon (ARA) from the patient sample P1 using PER-based approach (Fig. 4B). The mean fluorescence intensity of the beads treated with RNA fragments of the P1 sample was significantly higher (MFI_{P1}: 115) than the beads treated with the RNA fragments of P8 and H3 (MFI_{P8}: 15.1 and MFI_{H3}: 10). Consistent with this finding, the intensity of the adenine signal in the heterozygous R280K codon (G/A) of the P1 amplicon was also higher than the adenine signal of the P8 and H3 amplicons according to the Sanger sequencing (Fig. 4B).

CtDNAs exist alongside a vast background of wild-type DNAs, which are frequently distinguished by single-nucleotide changes with a variant allele frequency as low as 0.01% (Shin et al., 2023). To precisely detect and accurately quantify these single mutations, we further performed multicolor detection of the *KRAS* G12S mutation in the background of *KRAS* wild-type DNA fragments. For this, we first incubated the beads with biotinylated oligonucleotides and then added the WT and mutant *KRAS* fragments in different ratios in 1x PBS (WT:M; 1:1, 10:1, 100:1, 1000:1 and only WT) by keeping the WT fragment concentration at 100 nM. Then, we added corresponding PER concatemer probes in equal amounts designed for WT and mutant fragments distinctively, where the WT probe hybridizes with Alexa-488 labelled imager strands and the mutant probe hybridizes with Alexa-647 labelled imager strands. Flow cytometry data demonstrated that the mean fluorescence intensity obtained from mutant strands were highest at 1:1 ratio ($MFI_{G12S\ 50\%}$: 391) and decreased linearly down to 1000:1 ratio ($MFI_{G12S\ 10\%}$: 174, $MFI_{G12S\ 1\%}$: 126, $MFI_{G12S\ 0.1\%}$: 118) (Fig. 5). When there is no mutant strand in the solution the MFI obtained from Alexa-647 channel was 114, showing that we can detect the mutant strand even at the 0.1% of the WT strand concentration. In comparison, the MFI of WT strand at 1:1 ratio was 993 and the fluorescence signal did not change dramatically in all the other conditions ($MFI_{G12S\ 10\%}$: 1171, $MFI_{G12S\ 1\%}$: 1195, $MFI_{G12S\ 0.1\%}$: 1188 and MFI_{WT}: 1206). Overall, these results indicate that our PER-based detection approach can specifically detect the single mutations in target DNA and RNA strands and with the sensitivity of 0.1% of the concentration of the WT strands.

4. Conclusions

In summary, we developed a rapid, ultrasensitive and highly specific biosensor using the programmable PER-based fluorescence signal amplification approach and flow cytometry for the detection of cancer-associated nucleic acids and cancer-specific mutations. Our sensor demonstrated precise and accurate detection of both synthetic and natural nucleic acids extracted from human cells and plasma from breast cancer patients. The whole detection process can be completed in 3 h starting from biotinylation of the beads to the flow cytometry measurements and can take up to 7–8 h when pre-amplification, RNA synthesis and cleavage steps are required. The detection without pre-amplification is highly sensitive with a limit of detection reaching down to 27 fM using branched fluorescence signal amplification. Notably, we could precisely discriminate single nucleotide mutations frequently present in various cancer types, which shows the potential of our system for a quick detection of known mutations with in-house flow cytometers. Importantly, using a multi-color detection system, rare mutations can also be identified with a variant allele frequency as low as 0.1% concentration. Through pre-amplification of low abundant ctDNAs isolated from the plasma of breast cancer patient samples, we could also discriminate the single mutations. Overall, these results show the potential of our biosensor to be used in the clinics for early cancer detection, but also as a companion diagnostics test for personalized cancer therapies and disease monitoring. In a broader perspective, the use of developed biosensor can be expanded to detect nucleic acids and mutations in other disease conditions as well, in particular, cardiovascular, metabolic, inflammatory, autoimmune, infectious and neurodegenerative diseases.

CRediT authorship contribution statement

Samet Kocabey: Writing – original draft, Project administration, Methodology, Investigation, Data curation, Conceptualization. **Sarah Cattin:** Writing – review & editing, Methodology. **Isabelle Gray:** Writing – review & editing, Data curation. **Curzio Rüegg:** Writing – review & editing, Supervision, Funding acquisition.

Declaration of competing interest

The authors declare that they have no known competing financial interests or personal relationships that could have appeared to influence the work reported in this paper.

Data availability

Data will be made available on request.

Acknowledgements

This work was supported by the Swiss National Science Foundation through the National Center of Competence in Research Bio-Inspired Materials.

Appendix A. Supplementary data

Supplementary data to this article can be found online at https://doi.org/10.1016/j.bios.2024.116839.

References

Boskovic, F., Zhu, J., Tivony, R., Ohmann, A., Chen, K., Alawami, M.F., Dordevic, M., Ermann, N., Pereira-Dias, J., Fairhead, M., Howarth, M., Baker, S., Keyser, U.F., 2023. Simultaneous identification of viruses and viral variants with programmable DNA nanobait. Nat. Nanotechnol. 18 (3), 290–298.

Cattin, S., Fellay, B., Calderoni, A., Christinat, A., Negretti, L., Biggiogero, M., Badellino, A., Schneider, A.L., Tsoutsou, P., Pellanda, A.F., Ruegg, C., 2021. Circulating immune cell populations related to primary breast cancer, surgical removal, and radiotherapy revealed by flow cytometry analysis. Breast Cancer Res. 23 (1), 64.

Consortium, A.P.G., 2017. AACR Project GENIE: powering precision medicine through an international consortium. Cancer Discov. 7 (8), 818–831.

Domljanovic, I., Loretan, M., Kempter, S., Acuna, G.P., Kocabey, S., Ruegg, C., 2022. DNA origami book biosensor for multiplex detection of cancer-associated nucleic acids. Nanoscale 14 (41), 15432–15441.

Duffy, M.J., Crown, J., 2023. Circulating tumor DNA (ctDNA): can it be used as a pan-cancer early detection test? Crit. Rev. Clin. Lab Sci. 1–13.

Elazezy, M., Joosse, S.A., 2018. Techniques of using circulating tumor DNA as a liquid biopsy component in cancer management. Comput. Struct. Biotechnol. J. 16, 370–378.

Gomes, A.S., Trovao, F., Andrade Pinheiro, B., Freire, F., Gomes, S., Oliveira, C., Domingues, L., Romao, M.J., Saraiva, L., Carvalho, A.L., 2018. The crystal structure of the R280K mutant of human p53 explains the loss of DNA binding. Int. J. Mol. Sci. 19 (4).

He, Y., Zhan, Z., Yan, L., Wu, C., Wang, Y., Shen, C., Huang, K., Wei, Z., Lin, F., Ying, B., Li, W., Chen, P., 2024. Single-cell liquid biopsy of lung cancer: ultra-simplified efficient enrichment of circulating tumor cells and hand-held fluorometer portable testing. ACS Nano 18 (6), 5017–5028.

Huang, M., Xiang, Y., Chen, Y., Lu, H., Zhang, H., Liu, F., Qin, X., Qin, X., Li, X., Yang, F., 2023. Bottom-up signal boosting with fractal nanostructuring and primer exchange reaction for ultrasensitive detection of cancerous exosomes. ACS Sens. 8 (3), 1308–1317.

Kishi, J.Y., Lapan, S.W., Beliveau, B.J., West, E.R., Zhu, A., Sasaki, H.M., Saka, S.K., Wang, Y., Cepko, C.L., Yin, P., 2019. SABER amplifies FISH: enhanced multiplexed imaging of RNA and DNA in cells and tissues. Nat. Methods 16 (6), 533–544.

Kishi, J.Y., Schaus, T.E., Gopalkrishnan, N., Xuan, F., Yin, P., 2018. Programmable autonomous synthesis of single-stranded DNA. Nat. Chem. 10 (2), 155–164.

Kocabey, S., Chiarelli, G., Acuna, G.P., Ruegg, C., 2023. Ultrasensitive and multiplexed miRNA detection system with DNA-PAINT. Biosens. Bioelectron. 224, 115053.

Kosaka, N., Iguchi, H., Ochiya, T., 2010. Circulating microRNA in body fluid: a new potential biomarker for cancer diagnosis and prognosis. Cancer Sci. 101 (10), 2087–2092.

Kwapisz, D., 2017. The first liquid biopsy test approved. Is it a new era of mutation testing for non-small cell lung cancer? Ann. Transl. Med. 5 (3), 46.

Lazaro, A., Maquieira, A., Tortajada-Genaro, L.A., 2022. Discrimination of single-nucleotide variants based on an allele-specific hybridization chain reaction and smartphone detection. ACS Sens. 7 (3), 758–765.

Li, J., Dong, C., Gan, H., Gu, X., Zhang, J., Zhu, Y., Xiong, J., Song, C., Wang, L., 2023. Nondestructive separation/enrichment and rolling circle amplification-powered sensitive SERS enumeration of circulating tumor cells via aptamer recognition. Biosens. Bioelectron. 231, 115273.

Lone, S.N., Nisar, S., Masoodi, T., Singh, M., Rizwan, A., Hashem, S., El-Rifai, W., Bedognetti, D., Batra, S.K., Haris, M., Bhat, A.A., Macha, M.A., 2022. Liquid biopsy: a step closer to transform diagnosis, prognosis and future of cancer treatments. Mol. Cancer 21 (1), 79.

McConnell, E.M., Cozma, I., Mou, Q., Brennan, J.D., Lu, Y., Li, Y., 2021. Biosensing with DNAzymes. Chem. Soc. Rev. 50 (16), 8954–8994.

Mehlen, P., Puisieux, A., 2006. Metastasis: a question of life or death. Nat. Rev. Cancer 6 (6), 449–458.

O'Bryan, J.P., 2019. Pharmacological targeting of RAS: recent success with direct inhibitors. Pharmacol. Res. 139, 503–511.

Palacin-Aliana, I., Garcia-Romero, N., Asensi-Puig, A., Carrion-Navarro, J., Gonzalez-Rumayor, V., Ayuso-Sacido, A., 2021. Clinical utility of liquid biopsy-based actionable mutations detected via ddPCR. Biomedicines 9 (8).

Perakis, S., Speicher, M.R., 2017. Emerging concepts in liquid biopsies. BMC Med. 15 (1), 75.

Rafiee, S.D., Kocabey, S., Mayer, M., List, J., Ruegg, C., 2020. Detection of HER2(+) breast cancer cells using bioinspired DNA-based signal amplification. ChemMedChem 15 (8), 661–666.

Saka, S.K., Wang, Y., Kishi, J.Y., Zhu, A., Zeng, Y., Xie, W., Kirli, K., Yapp, C., Cicconet, M., Beliveau, B.J., Lapan, S.W., Yin, S., Lin, M., Boyden, E.S., Kaeser, P.S., Pihan, G., Church, G.M., Yin, P., 2019. Immuno-SABER enables highly multiplexed and amplified protein imaging in tissues. Nat. Biotechnol. 37 (9), 1080–1090.

Shimoi, T., Hamada, A., Yamagishi, M., Hirai, M., Yoshida, M., Nishikawa, T., Sudo, K., Shimomura, A., Noguchi, E., Yunokawa, M., Yonemori, K., Shimizu, C., Kinoshita, T., Fukuda, T., Fujiwara, Y., Tamura, K., 2018. PIK3CA mutation profiling in patients with breast cancer, using a highly sensitive detection system. Cancer Sci. 109 (8), 2558–2566.

Shin, S., Han, S., Kim, J., Shin, Y., Song, J.J., Hohng, S., 2023. Fast, sensitive, and specific multiplexed single-molecule detection of circulating tumor DNA. Biosens. Bioelectron. 242, 115694.

Siravegna, G., Marsoni, S., Siena, S., Bardelli, A., 2017. Integrating liquid biopsies into the management of cancer. Nat. Rev. Clin. Oncol. 14 (9), 531–548.

Soleymani, L., Fang, Z., Lam, B., Bin, X., Vasilyeva, E., Ross, A.J., Sargent, E.H., Kelley, S. O., 2011. Hierarchical nanotextured microelectrodes overcome the molecular transport barrier to achieve rapid, direct bacterial detection. ACS Nano 5 (4), 3360–3366.

Song, P., Wu, L.R., Yan, Y.H., Zhang, J.X., Chu, T., Kwong, L.N., Patel, A.A., Zhang, D.Y., 2022. Limitations and opportunities of technologies for the analysis of cell-free DNA in cancer diagnostics. Nat. Biomed. Eng. 6 (3), 232–245.

Sorenson, G.D., Pribish, D.M., Valone, F.H., Memoli, V.A., Bzik, D.J., Yao, S.L., 1994. Soluble normal and mutated DNA sequences from single-copy genes in human blood. Cancer Epidemiol. Biomarkers Prev. 3 (1), 67–71.

Sun, Y., Sun, J., Xiao, M., Lai, W., Li, L., Fan, C., Pei, H., 2022. DNA origami-based artificial antigen-presenting cells for adoptive T cell therapy. Sci. Adv. 8 (48), eadd1106.

Tanaka, N., Kanatani, S., Tomer, R., Sahlgren, C., Kronqvist, P., Kaczynska, D., Louhivuori, L., Kis, L., Lindh, C., Mitura, P., Stepulak, A., Corvigno, S., Hartman, J., Micke, P., Mezheyeuski, A., Strell, C., Carlson, J.W., Fernandez Moro, C., Dahlstrand, H., Ostman, A., Matsumoto, K., Wiklund, P., Oya, M., Miyakawa, A., Deisseroth, K., Uhlen, P., 2017. Whole-tissue biopsy phenotyping of three-dimensional tumours reveals patterns of cancer heterogeneity. Nat. Biomed. Eng. 1 (10), 796–806.

Vallee, A., Le Loupp, A.G., Denis, M.G., 2014. Efficiency of the Therascreen(R) RGQ PCR kit for the detection of EGFR mutations in non-small cell lung carcinomas. Clin. Chim. Acta 429, 8–11.

Wan, J.C.M., Massie, C., Garcia-Corbacho, J., Mouliere, F., Brenton, J.D., Caldas, C., Pacey, S., Baird, R., Rosenfeld, N., 2017. Liquid biopsies come of age: towards implementation of circulating tumour DNA. Nat. Rev. Cancer 17 (4), 223–238.

Williams, Z., Ben-Dov, I.Z., Elias, R., Mihailovic, A., Brown, M., Rosenwaks, Z., Tuschl, T., 2013. Comprehensive profiling of circulating microRNA via small RNA sequencing of cDNA libraries reveals biomarker potential and limitations. Proc. Natl. Acad. Sci. U. S. A. 110 (11), 4255–4260.

Yu, Z., Pan, L., Ma, X., Li, T., Wang, F., Yang, D., Li, M., Wang, P., 2023. Detection of SARS-CoV-2 RNA with a plasmonic chiral biosensor. Biosens. Bioelectron. 237, 115526.

Zhang, Z., Guiley, K.Z., Shokat, K.M., 2022. Chemical acylation of an acquired serine suppresses oncogenic signaling of K-Ras(G12S). Nat. Chem. Biol. 18 (11), 1177–1183.